

a NASA facsimile reproduction

OF

MSC-3441

REPRODUCED FROM MICROFICHE

by the

NASA Scientific and Technical Information Facility



KIRTLAND AFB
AFWL (W1
LOAN COPY: R1

0152384



TECH LIBRARY KAFB, NM



X-621-68-329
PREPRINT

NASA TM X- 63326

A DIRECT MEASUREMENT
OF ION COMPOSITION
AND CONCENTRATION
IN THE DAYTIME F₂-REGION

GPO PRICE \$ _____

CSFTI PRICE(S) \$ _____

Hard Copy (HC) 3.00

Microfiche (MF) .65

11-653 JUN 65

H.C. BRINTON
M.W. PHARO, III
H.G. MAYR
H.A. TAYLOR, JR.

FACILITY FORM 602	25-341-1	(TITLE)
	34	(PAGES)
	TMX 63326	(NASA OR TAX OR AD NUMBER)
		(CATEGORY)

AUGUST 1968



GODDARD SPACE FLIGHT CENTER
GREENBELT, MARYLAND



X-621-68-329
PREPRINT

A DIRECT MEASUREMENT OF ION COMPOSITION AND
CONCENTRATION IN THE DAYTIME F₂-REGION

by

H. C. Brinton, M. W. Pharo, III,
H. G. Mayr*, and H. A. Taylor, Jr.

Laboratory for
Atmospheric and Biological Sciences
Goddard Space Flight Center
Greenbelt, Maryland

*NAS - NRC Resident Research Associate, now with NASA



CONTENTS

	<u>Page</u>
ABSTRACT	v
INTRODUCTION	1
PAYLOAD INSTRUMENTATION	1
THE ION SPECTROMETER	2
RESULTS	3
Ion Current Data	3
Derivation of Ion Concentration Profiles	3
Altitude Variation of Ion Composition	4
DISCUSSION	6
Chemical Equilibrium Distribution of H^+	6
Chemical Equilibrium Distribution of He^+	9
Evidence of the Dynamic State of the Topside Ionosphere	10
ACKNOWLEDGMENTS	17
REFERENCES	18

A DIRECT MEASUREMENT OF ION COMPOSITION AND
CONCENTRATION IN THE DAYTIME F_2 -REGION

by

H. C. Brinson, M. W. Pharo, III,
B. G. Mavr*, and H. A. Taylor, Jr.

ABSTRACT

The positive ion mass spectrometer on the Geoprobe (NASA # 25) rocket measured the concentrations of O^+ , N^+ , H^+ , He^+ , NO^+ , O_2^+ and N_2^+ between 200 km and peak altitude, 630 km, at 1300 EST on March 2, 1966 above Wallops Island, Virginia. O^+ was the dominant ion throughout the altitude range, reaching a maximum concentration of 5×10^4 ions cm^{-3} at 260 km. H^+ was first detected at 230 km and increased in concentration to 7×10^3 ions cm^{-3} at peak altitude. The H^+/He^+ ratio was never lower than 6.0, the value at 420 km. NO^+ and O_2^+ were important constituents at 200 km, the concentration of each being 5×10^4 ions cm^{-3} ; they fell off rapidly above this altitude. He^+ was in photochemical equilibrium up to 400 km with a rate coefficient of $0.5 \times 10^{-10} cm^3 sec^{-1}$ for charge transfer with N_2 . In agreement with laboratory measurement, H^+ was in charge exchange equilibrium with O^+ , O and H up to 450 km, the temperature derived for the neutrals in both the He^+ and H^+ chemistry was 750 K, which agrees with T_e measured by companion neutral particle sensors. From the variation of H^+/O^+ and an O^+ distribution based on a simultaneous EUV measurement, a profile of H^+ in the chemical equilibrium region was calculated. The

*NAS-NRC Resident Research Associate, now with NASA

derived H concentrations are higher than the Jacchia 1964 Model predictions, and agree with Explorer 32 spectrometer results. Analysis indicates that N⁺ was not in diffusive equilibrium at 300 km, and that a downward neutral wind $V_0 = -25$ m/sec is required to produce the observed N⁺ scale height at this altitude. Distributions of O⁺ and H⁺ above 300 km were derived by solving the continuity equations along field lines, an upward H⁺ flux of 1.5×10^7 cm²/sec was required to reproduce the observed profiles, indicating that the critical flux is at least an order of magnitude higher than previously believed.

A DIRECT MEASUREMENT OF ION COMPOSITION AND CONCENTRATION IN THE DAYTIME F₂-REGION

INTRODUCTION

The Geoprobe (NASA 827) was launched from Wallops Island, Virginia at 1300 EST on March 2, 1966. An Argon D1 rocket carried the pressurized cylindrical payload containing six experiments to an altitude of 630 km to measure the vertical profiles of electron density and temperature, neutral gas density, composition, and temperature, and ion concentration and composition. Valuable correlative data were obtained from the concurrent flight of an Aerobea rocket (NASA 496), launched two minutes before the Geoprobe to measure incoming solar EUV radiation (Fichtel, 1967). We report here the results obtained by the Geoprobe ion mass spectrometer and interpret these results using portions of data obtained by the other experiments.

PAYLOAD INSTRUMENTATION

The following experiments comprised the Geoprobe payload (Figure 1): electrostatic probe, planar retarding potential analyzers for ions and electrons, Bennett ion mass spectrometer, CW propagation experiment (two-frequency dispersive Doppler technique), two laser Alpert gauges, and a neutral particle magnetic mass spectrometer. Additional instrumentation included an optical aspect system, two and three magnetometers, and supporting electronics.

The ion spectrometer and the ion retarding potential analyzer were mounted at the forward end of the payload as shown in Figure 1. To provide a uniform

electric field, an aluminum guard ring with a gridded opening over each instrument orifice covered the end of the payload and was insulated from it.

THE ION SPECTROMETER

The Bennett ion spectrometer consisted of a single instrument package containing both the ceramic sensor tube and electronics. The tube was similar in construction to those previously flown on rockets and satellites as described by Taylor et al. (1963, 1965). The theory of Bennett spectrometer operation has been rigorously described in the literature (C. Y. Johnson, 1969), so only those characteristics particular to the Geoprobe instrument will be described here.

The sensor, a 5-3 cycle 5 mm tube, was mounted with its axis parallel to the payload axis. The guard ring (G_1) was biased on alternate mass scans at 0 and -4 volts, the negative potential producing no measurable change in collected ion current at 300 km, but increasing the current by a factor of ~ 2 at peak altitude. The trifurcated accelerating voltage (V_a) scanned the mass range from 0.5 to 4.6 amu, and then from 3.1 to 3 amu with a period of 3.8 seconds by switching the rf from 9.6 MHz to 3.3 MHz. The stopping voltage (V_s), which regulates the flow of ions to the spectrometer collector, was alternated between 48 and 57 volts, the change occurring every two mass scans. The stepping guard ring voltage and V_s thereby provide four experiment operating modes and corresponding sensitivities.

RESULTS

Ion Current Data

Between 1301 L (EST) at an altitude of 177 km, four secondary flow nose cone ejection and 1311 L at 162 km during payload descent, 175 mass scans containing ion current peaks were recorded. Peaks were detected at m/z 1, 4, 11, 16, 18, 28, 36, and 72 amu which are respectively atomic hydrogen, helium, atomic nitrogen and oxygen, water, molecular nitrogen, nitric oxide, and molecular oxygen. Smooth curves representing the ion current profiles measured in the 0 to -6 volt V_s mode are shown in Figure 2. The curves have been smoothed to remove the effects of payload jarring which occurred with a half amplitude of $\sim 10^\circ$ and a scatter of approximately 15% in the points of fit. At each point of jarring a correction was applied to the measured H^+ ion current to account for mass discrimination in the spectrometer analyzer. Corrected values of the measured ion currents, used in deriving profiles of ambient ion concentration, are shown in Figure 2. Ion concentration during descent causing the spectrometer to measure in the payload wake data from this portion of the flight are not presented.

Derivation of Ion Concentration Profiles

The conversion from ion current to ambient ion concentration was performed by normalizing the total ion current profile (I_t) to a profile of the total ion concentration (N_t), the latter having been determined by other Geoprobe charged particle experiments. The N_t profile in Figure 3 was obtained by averaging the electron density distributions obtained by the electrostatic probe (Brace et al., 1968) and CW propagation experiment (S. J. Bauer, private communication) and the ion density profile obtained by the ion retarding potential analyzer (F. L. Donley,

private communication). The necessary assumption that charge neutrality existed at all altitudes was well supported by the data. It may be seen that the O^+ and N^+ profiles are similar in form, but that they diverge at high and low altitudes. At high altitudes the divergence was caused by the decreasing vertical component of payload velocity and increasing spectrometer angle-of-attack, while the deviation below 300 kilometers was the result of "shadowing" of the payload by the ejected nose cone. The ion current measured by the retarding potential analyzer adjacent to the ion spectrometer exhibited similar behavior (J. L. Donley, private communication). In deriving the altitude profiles of the individual ion constituents shown in Figure 4, it was assumed that the ratios of the measured ion currents accurately reflected the ratios of the ambient concentrations (except for H^+ , as stated earlier).

It should be pointed out that Brace et al. (1968) have reported that the electron density they measured during payload descent was 30% lower than that measured on ascent. The difference is attributed to a horizontal density gradient, detected because of the Geoprobe's large horizontal range (871 km). Our ion data covers obtained on ascent and have been normalized to the ascent concentration distribution. It is probable, then, that the ion profiles above 200 km (where vertical/horizontal velocity ratio is low) do not represent pure altitude variations, but deviate from the true distributions by as much as 30%.

Altitude Variation of Ion Composition

The variation with altitude of the individual ion concentrations is presented in Figure 4. O^+ was the dominant constituent throughout the observed altitude range, its concentration reaching a maximum of approximately 5×10^5 ions/cm³ (200 km). The N^+ profile was similar to that of O^+ , the $O^+ : N^+$ ratio being

70 at I_{max} (270 km) and decreasing to 20 at peak altitude. H^+ was first detected at 200 km; its concentration increased with altitude to a value of 7×10^3 ions/cm³ at peak. The concentration of H^+ never exceeded that of O^+ ($H^+ : O^+$ ratio being smallest) (1200 : 1) at peak, and was 50 : 1 at peak altitude. The minor role played by H^+ during this period of low solar activity is supported by extensive ion composition data obtained near the time by several other spacecraft on the OGO-2 Explorer (1964) and Explorer 32 (Brace et al., 1968) satellites.

The important features of the NO^+ and N_2^+ ion currents are also shown with increasing altitude. Figure 4 shows that during payload descent (ascent) shows that both NO^+ and N_2^+ were present at a similar concentration level at 200 km, although agreement of the two ion composition ratios is not perfect. Molecular concentrations below 200 km with altitude to about 100 km show a gradual change of ratio here is observed. The reason for this change is not understood, and the three profiles presented above this level to minimize our uncertainty. The molecular ion currents measured at high altitude (> 300 km) are the limit of spectrometer sensitivity and the signal/noise ratio was poor. A possible explanation is that the molecular ions detected above 300 km were not atmospheric, but instead resulted from ionization of contaminants outgassed from the payload.

No concentration profile for H_2O^+ is included in Figure 4 corresponding to the current profile in Figure 2, since we believe this ion was not atmospheric, but resulted from charge exchange of H_2O outgassed from the payload with ambient O^+ .

DISCUSSION

The ion composition of the atmosphere is the product of chemical and transport processes. Chemical reactions dominate at low altitudes where production and loss rates, which depend proportionally on neutral and charged particle concentrations, are high. With increasing altitude the significance of chemical reactions decreases, while transport processes become more important due to the increase of diffusion coefficients which depend inversely on particle concentrations. Thus, for a given ion species, chemical equilibrium holds at lower altitudes, while diffusive equilibrium governs the ion distribution at higher altitudes. Both types of equilibrium provide simple relationships between the ion distributions and gas or plasma temperature, we will evaluate certain of these relationships using the *Geoprobe* data.

Chemical Equilibrium Distribution of H^+

J. S. Johnson (1960) recognized the significance of the charge exchange reaction



in the formation of the protonosphere. Hanson and Ortenburger (1961) discussed the hydrogen ion distribution in some detail and showed that H^+ approaches the chemical equilibrium distribution

$$H^+ = \frac{g}{B} \frac{O^+ H}{O} \quad (2)$$

at altitudes below 700 km. Relation (2), in conjunction with *Geoprobe* measurements of H^+ and O^+ , leads to the derivation of the neutral gas temperature T_g ,

6

if H and O are assumed to be in diffusive equilibrium. Equation (2) can be written in the form

$$\frac{H}{O} = \frac{g}{k T_g} \frac{H}{O} \quad (2a)$$

thereby relating the ratio of neutral H and O, whose altitude variation is only a function of T_g , to the measured ratio of H^+ and O^+ . The scale height, h , of the ion ratio is defined by

$$h = \frac{z}{O^+} \quad (3)$$

in which z is geopotential altitude given by

$$z = \int_{h_0}^h \frac{g}{g_0} dh$$

where g_0 is the gravitational acceleration at a reference height h_0 , and g is the acceleration at altitude h . The scale height of the ion ratio is thus related through (2a) to the neutral constituents as follows

$$\frac{1}{h} = \frac{g}{z} \ln \left(\frac{H}{O} \right) = \frac{1}{H} \frac{H}{z} = \frac{1}{O} \frac{O}{z} \quad (4)$$

The equations of diffusive equilibrium for H and O are

$$\frac{1}{H} \frac{H}{z} = \frac{1}{T_g} \frac{T_g}{z} = \frac{m_H g}{k T_g} = 0 \quad \text{and} \quad (5)$$

$$\frac{1}{O} \frac{O}{z} = \frac{1}{T_g} \frac{T_g}{z} = \frac{m_O g}{k T_g} = 0 \quad (6)$$

7

where m_H and m_O are the masses of H and O respectively. Substituting (5) and (6) into (4) leads to the relation

$$\frac{1}{h} = \frac{g}{kT_e} (m_O - m_H) \quad (7)$$

showing that the scale height of the observed ion ratio is only a function of T_e . Although allowance was made for a temperature gradient in (5) and (6), h evidently does not depend on it. Consequently it should be possible to deduce altitudinal temperature variations by determining the scale height of the H^+/O^+ ratio at different altitudes.

The altitude profile of H^+/O^+ measured by the Geoprobe spectrometer is the solid line in Figure 5. Applying relation (7) to the best-fit dashed line we derive an atmospheric temperature of 750° K, a value in reasonable agreement with temperatures determined by the Geoprobe neutral particle mass spectrometer (Cooley and Reber, 1968) and pressure gauges (Pelz and Newton, 1968). At 450 km the ion ratio deviates from a straight line indicating that relation (2a), and thus chemical equilibrium, no longer holds. This is expected, as the diffusion process which tends to decrease the H^+ concentration becomes significant at higher altitudes.

The distribution of neutral hydrogen in the chemical equilibrium region has been derived using the measured H^+/O^+ ratio (Figure 5), an altitude profile of O , based on the near simultaneous measurement of solar EUV by Hall et al., 1967, and relation (2a). The O profile and calculated H distribution are shown in Figure 6. The O distribution was obtained by extrapolating upward the low altitude O data of Hall et al. (circles in Figure 6), assuming diffusive

equilibrium and employing the derived T_e of 750° K. Reasonable agreement is shown between this profile and the dashed O distribution from the most appropriate model atmosphere of Jacchia (1964) (1200 LT, $F_{10.7} = 90$, and $T_e = 850°$ K). The calculated H distribution, shown as a solid line in the chemical equilibrium region, is a factor of approximately five higher in concentration than the Jacchia prediction, and is in general agreement with the measurements by Reber et al. (1968), employing the neutral particle mass spectrometers on Explorer 32. A diffusive equilibrium profile for H at 750° K, the thin solid line in Figure 6, was located by normalization to the calculated H distribution and fits the latter well.

Chemical Equilibrium Distribution of He^+

The altitude profile of He^+ measured by Geoprobe is shown in Figure 7. Atmospheric helium ions are produced by photoionization of neutral helium and lost by charge transfer reactions with molecular constituents. Bauer (1966) pointed out that, according to laboratory measurements, the reaction



would be expected to be the most important loss process for He^+ in the chemical equilibrium region, with a rate coefficient k_1 of $10^{-9} \text{ cm}^3 \text{ sec}^{-1}$ (Ferguson et al., 1964). He found this value of k_1 inconsistent, however, with the rocket spectrometer measurements of He^+ and N^+ by Pokhunkov (1963), which suggested an upper limit for the coefficient of $10^{-11} \text{ cm}^3 \text{ sec}^{-1}$. Our study of the Geoprobe results indicates that He^+ is in photochemical equilibrium up to 400 km and that the rate coefficient determined from flight data agrees with the laboratory measurement.

N^+ and O^+ , and N^+ and O , respectively. Combining the Geoprobe ion composition measurements with T_e data from the electrostatic probe in the same payload

Brace et al., 1968, allows us to evaluate equation (11) at 300 km where T_e can be assumed almost equal to T_a . The following values are obtained for the terms in (11): the first term on the right hand side $+1.6 \times 10^{-10} \text{ cm}^{-3}$, the second $-3.7 \times 10^{-10} \text{ cm}^{-3}$, and the third $-1.6 \times 10^{-8} \text{ cm}^{-3}$. Thus for diffusive equilibrium, where $V_{N^+} - V_{O^+} = V_{N^+} - V_{O^+} = 0$, the N^+ distribution is given by

$$\frac{1}{N^+} \frac{dN^+}{dz} = -2.0 \times 10^{-7} \text{ cm}^{-1} \quad (11a)$$

meaning that N^+ should increase with altitude with a scale height of 50 km. The Geoprobe observation indicates, however, that N^+ is decreasing at 300 km with a scale height of 180 km, yielding a value of $-5.5 \times 10^{-8} \text{ cm}^{-1}$ for (11a). Thus we agree with the suggestion by Bauer (1966), based on his analysis of the Pokhunkov (1963) data, that diffusive equilibrium may not hold for N^+ at 300 km, we therefore conclude that the effects of the drag terms in (11) must be considered.

The transport velocity V_{N^+} can be estimated by considering the continuity equation

$$k_1 \text{He}^+ + N_2^+ - k_2 N^+ + O_2^+ - \frac{1}{h} (V_{N^+} N^+) = 0 \quad (12)$$

In which reaction (8) is assumed the source of N^+ and the reaction



with $k_2 = 5 \times 10^{-10} \text{ cm}^3 \text{ sec}^{-1}$, is assumed the dominant N^+ loss process

Fehsenfeld et al., 1965). By integration of (12) the ion flux $V_{N^+} N^+$ is given by

$$V_{N^+} N^+ = k_1 \int_{h_0}^z \text{He}^+ + N_2^+ - k_2 N^+ + O_2^+ dz \quad (14)$$

if it is assumed that at high altitudes V_{N^+} approaches zero. It was demonstrated earlier that He^+ is in chemical equilibrium at 100 km, increasing with altitude according to a distribution described by (9). Above this altitude He^+ approaches diffusive equilibrium and starts to decrease, as shown in Figure 4. By substituting (9) into (14) we can estimate an upper limit for the first integral

$$k_1 \int_{h_0}^z \text{He}^+ + N_2^+ = 2.2 \times 10^{-10} \exp(-z/h_0) \quad (15)$$

where h_0 is the scale height. The first term of integral in (14) can be evaluated by noting that the observed scale height of N^+ at 300 km is almost constant, thus yielding

$$k_2 \int_{h_0}^z N^+ dz = k_2 N^+ h_0 = O_2^+ + \frac{k_1 N^+ h_0}{N^+} = 5.5 \times 10^{-8} \text{ cm}^{-3} \quad (16)$$

where h_0 is the scale height of O_2^+ . Expression (16) was evaluated by assuming $O_2^+ = 8 \times 10^{-10} \text{ cm}^{-3}$ obtained by extrapolating the data of Hall et al., 1967. Comparison of (15) with (16) indicates that the loss rate of N^+ above 300 km exceeds the production rate, resulting in an upward N^+ flux of the order of $V_{N^+} N^+ = 1 \times 10^{-7} \text{ cm}^{-3} \text{ sec}$ which corresponds to a velocity of

$$V_{N^+} = 5 \text{ m/sec} \quad (17)$$

at 300 km

Having thus determined the approximate value of V_{O^+} , we next derive an estimate of V_{O^+} . Assuming that the F_2 region is stationary (negligible temporal variation) we can, in a manner similar to that for N^+ , calculate the O^+ flux by integrating the continuity equation above 300 km. In this altitude range dissociative recombination is negligible, thus only photoionization of O has to be considered as a source of O^+ . Assuming the photoionization rate to be 8×10^4 cm^2/sec at 300 km (Hinteregger et al., 1965), the calculation yields a downward flux of 4×10^8 cm^2/sec , corresponding to a velocity of

$$V_{O^+} = 10^{-7} \text{ sec} \quad (19)$$

at 300 km.

Substituting (17) and (18) into the O^+-N^+ drag term of (11) (with $v_{O^+} = 5 \times 10^{-29}$ $\text{gm cm}^3/\text{sec}^{-1}$) reduces the term $1/N^+ \cdot N^+ \cdot v_z$ from its diffusive equilibrium value of $+2.0 \times 10^{-11}$ cm^{-1} to zero, which is in better agreement with observation. To further decrease the scale height, bringing it closer to the measured value, the drag term in (11) for the interaction between O^+ and N^+ is considered. Assuming $v_{O^+} = 1 \times 10^{-32}$ $\text{gm cm}^3/\text{sec}^{-1}$, a downward wind $V_{O^+} = -25$ m/sec is required to decrease the value of (11a) to -5.5×10^{-11} cm^{-1} , thereby reproducing the measured scale height of N^+ at 300 km. This result is in excellent agreement with the conclusion of Brace et al. (1968), who based their wind estimate on the observed O^+ scale height. We conclude that the distribution of N^+ in the topside ionosphere may be strongly controlled by drag interactions arising from the transport of charged and neutral constituents.

On the basis of this result the alternative explanation for the distribution of O^+ (Brace et al., 1968) involving an upward flux of O^+ can be ruled out. The

latter would require a positive upward velocity $V_{O^+} = +15$ m/sec, which would increase the value of $1/N^+ \cdot N^+ \cdot v_z$ to $+3.3 \times 10^{-11}$ cm^{-1} , thus requiring an even greater increase of N^+ with altitude in contradiction with the observed distribution.

The two major ions in the topside ionosphere at the time of the Geoprobe measurement were O^+ , dominant between 180 and at least 350 km, and H^+ , which became increasingly significant and finally dominant at higher altitudes. These constituents determined the altitudinal variation of electron density and plasma temperature during this period of low solar activity. In order to better understand the O^+ and H^+ altitude profiles we have attempted to reproduce the distributions theoretically.

Considering charge exchange reaction (1), photoionization of O and H, and diffusion processes, the continuity equations for H^+ , O^+ and N_2^+ were solved simultaneously above 300 km in the field tube corresponding to the geomagnetic location of the Geoprobe measurement, following the technique of Mayr et al. (1967). It was assumed for symmetry that the particle flux is zero at the equator, and that diffusion across field lines can be neglected. The measured O^+ concentration at 300 km was adopted as a boundary condition and H^+ was assumed to be in chemical equilibrium with O^+ , O and H below 400 km according to relation (2). The ion and electron temperatures used in the particle continuity equations were derived from the energy continuity equations, in which the energy input rates were adjusted to reproduce the observed electron temperature distribution (Brace et al., 1968). The concentrations of H and O at 300 km were taken from the derived H profile (Figure 6) and Jacchia's Model, respectively, and it was assumed that these constituents are in diffusive equilibrium at a gas temperature

of 750°K. Following Brace et al. (1968), and considering the neutral wind conclusion derived earlier, a wind of $V_z = 25$ m/sec was also assumed.

The H^+ and O^+ distributions were first computed assuming no proton flux, the resulting profiles being the dashed lines in Figure 8. The theoretical O^+ profile agrees with the measured distribution up to 500 km, while beyond this altitude it differs by ~30%. This difference could result from a distortion of the measured profile by a horizontal concentration gradient as discussed in an earlier section. For the H^+ distribution the agreement between measurement and theory is acceptable only up to 150 km. Above this altitude a significant deviation is apparent. The calculated H^+ concentration at 600 km is almost a factor of three higher than the measured value, a difference not likely caused by a horizontal density gradient. We have assumed that the difference is attributable to an upward flux of protons and have performed a second calculation assuming an H^+ flux of $1.5 \times 10^8/cm^2sec$; the results are shown as solid lines in Figure 8. While the O^+ distribution is only slightly affected by the introduction of this flux, the new H^+ profile is now close to the measured points over the entire altitude range, the difference at 600 km being less than 30%.

We conclude, then, that an upward flux of protons is required to explain the Geoprobe H^+ profile, and that the critical flux, the upper limit to the magnitude of the proton flow, must be at least of the order of $1.5 \times 10^8/cm^2sec$. This result indicates that the protonosphere can be supplied by ion fluxes an order of magnitude higher than previously assumed (Hanson and Patterson, 1964; Geisler, 1967) a fact that could possibly explain the maintenance of the nighttime F_2 -layer. This increase in the estimated critical flux is due to (1) the significantly

higher hydrogen concentrations derived from O^+ ion composition data, and (2) the high transparency of the O^+ ion barrier to H^+ because of the relatively high plasma temperatures measured during the Geoprobe flight.

ACKNOWLEDGMENTS

The authors gratefully acknowledge the contributions of J. S. Burch to the development of both the ion spectrometer and the total Geoprobe payload, which are further indebted to C. R. Smith and P. J. Conner, who guided the design, calibration, and testing of the ion spectrometer. We also wish to thank Dr. S. J. Bauer and J. E. Donnelly for the use of their unpublished data.

REFERENCES

- Bauer, R. J., Chemical processes involving helium ions and the behavior of atomic nitrogen ions in the upper atmosphere, J. Geophys. Res., 71, 1508-1511, 1966.
- Brace, L. H., J. A. Findlay, and H. G. Mayr, Electron measurements bearing on the energy and particle balance of the upper F-region, submitted to J. Geophys. Res., 1968.
- Brinton, H. C., R. A. Pickeath, and H. A. Taylor, Jr., Seasonal dependence of the diurnal variation of atomic oxygen ion composition obtained from Explorer 72, paper presented at the American Geophysical Union meeting, Washington, D. C., April 1968.
- Cooler, J. E. and C. A. Reber, Neutral atmospheric composition measurement between 180 and 420 km from the Geoprobe rocket mass spectrometer, submitted to J. Geophys. Res., 1968.
- Fehsenfeld, F. C., A. L. Schmeltekopf, and E. E. Ferguson, Some measured rates for oxygen and nitrogen ion-molecule reactions of atmospheric importance including $O^+ + N_2$, $NO^+ + N$, Planet. Space Sci., 13, 219-223, 1965.
- Ferguson, E. E., F. C. Fehsenfeld, D. B. Dunkin, A. L. Schmeltekopf, and H. I. Schiff, Laboratory studies of helium ion loss processes of interest in the ionosphere, Planet. Space Sci., 12, 1169-1172, 1964.
- Gelsler, J. E., On the limiting daytime flux of ionization in the protonosphere, J. Geophys. Res., 72, 81-85, 1967.
- Hall, L. A., C. W. Chagnon, and H. E. Hinteregger, Daytime variations in the composition of the upper atmosphere, J. Geophys. Res., 72, 3425-3427, 1967.
- Hinteregger, H. F., L. A. Hall, and G. Schmidtke, Solar XUV radiation and neutral particle distribution in July 1963 thermosphere, Space Research V, edited by P. Muller, North-Holland Publishing Co., Amsterdam, 1175-1190, 1965.
- Holmes, J. C., C. Y. Johnson, and J. M. Young, Ionospheric chemistry, Space Research V, edited by P. Muller, North-Holland Publishing Co., Amsterdam, 756-766, 1965.
- Hanson, W. B., and I. B. Ortenburger, The coupling between the protonosphere and the normal F-region, J. Geophys. Res., 66, 1425-1435, 1961.
- Hanson, W. B. and T. N. L. Patterson, The maintenance of the night-time F-layer, Planet. Space Sci., 12, 979-997, 1964.
- Jacchia, L. G., Static diffusion models of the upper atmosphere with empirical temperature profiles, Special Report 170, Smithsonian Institution Astrophysical Observatory, Cambridge, Mass., December, 1964.
- Johnson, C. Y., Bennett radio frequency spectrometer, Encyclopedia of Spectroscopy, edited by G. L. Clark, Reinhold Publishing Corp., New York, 587-598, 1960.

Johnson, F. S., The ion distribution above the F_2 -maximum, J. Geophys. Res., 65, 577-584, 1960.

Mayr, H. G., L. H. Brace, and G. S. Dunham, Ion composition and temperature in the topside ionosphere, J. Geophys. Res., 72, 4391-4403, 1967.

Nicolet, M., Helium, an important constituent in the lower exosphere, J. Geophys. Res., 66, 2263-2264, 1961.

Pelz, D. T. and G. P. Newton, Midlatitude neutral thermosphere density and temperature measurements, submitted to J. Geophys. Res., 1968.

Pokhunkov, A. A., Mass-spectrometric measurements of the distribution of He^+ , N^+ , O^+ , NO^+ , and O_2^+ ions in the earth's atmosphere up to a height of 430 km, Kosmich. Issled. (J. Space Flight Res.), 1, 267-270, 1963.

Reber, C. A., J. E. Cooley, and D. N. Harpold, Upper atmosphere hydrogen and helium measurements from the Explorer 32 satellite, Space Research VIII, North-Holland Publishing Co., Amsterdam, 993-995, 1968.

Taylor, H. A., Jr., L. H. Brace, H. C. Brinton, and C. R. Smith, Direct measurements of helium and hydrogen ion concentration and total ion density to an altitude of 940 kilometers, J. Geophys. Res., 68, 5339-5347, 1963.

Taylor, H. A., Jr., and H. C. Brinton, Atmospheric ion composition measured above Wallops Island, Virginia, J. Geophys. Res., 66, 2587-2588, 1961.

Taylor, H. A., Jr., H. C. Brinton, M. W. Pharo, III, and N. K. Rahman, Thermal ions in the exosphere: evidence of solar and geomagnetic control, J. Geophys. Res., in press, 1968.

Taylor, H. A., Jr., H. C. Brinton, and C. R. Smith, Positive ion composition in the magnetoliosphere obtained from the OGO-A satellite, J. Geophys. Res., 70, 5769-5781, 1965.

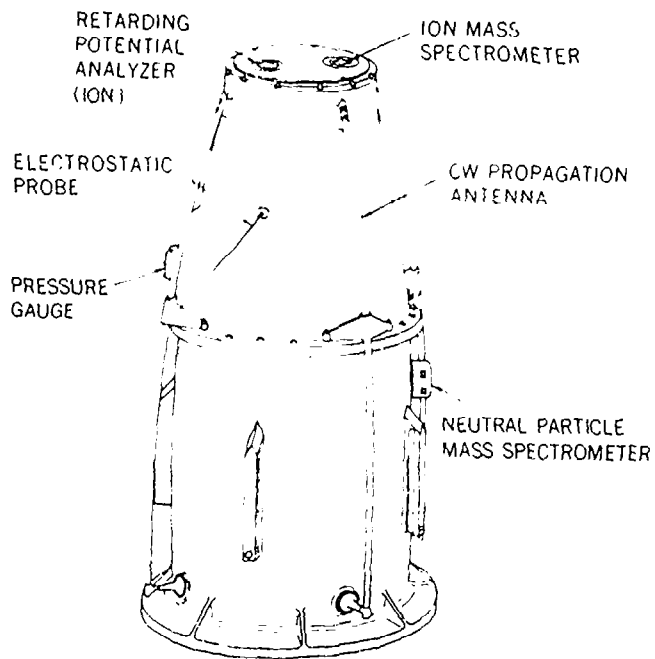


Figure 1.-Geoprobe (NASA 8 25) payload, showing instrument locations

22

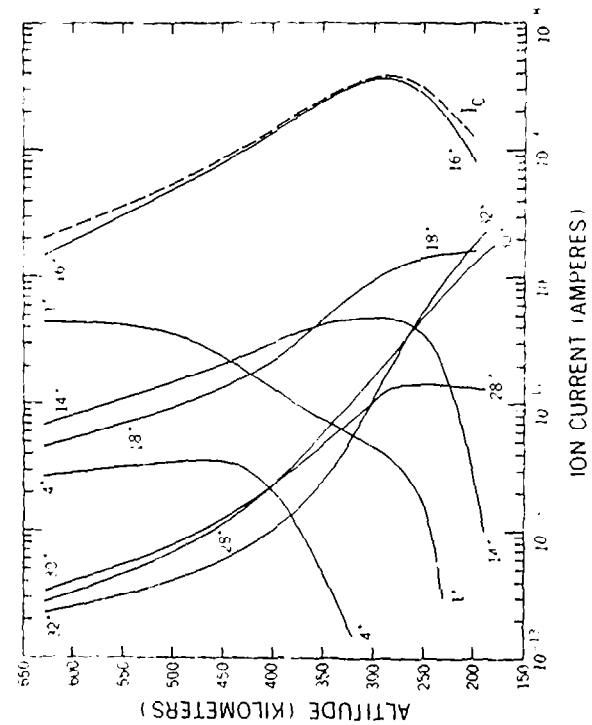


Figure 2.-Smooth ion current profiles drawn through the data points obtained during rocket ascent. The dashed curve, I_c , is the sum of the measured currents.

23

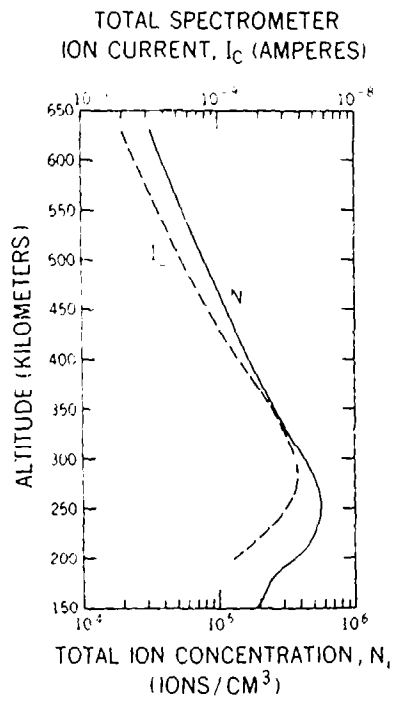


Figure 3. Profiles used for conversion of measured ion current to ambient ion concentration. The ion current profile I_C (from Figure 2) was normalized to the total ion concentration profile, N_i , determined by companion Geoprobe experiments.

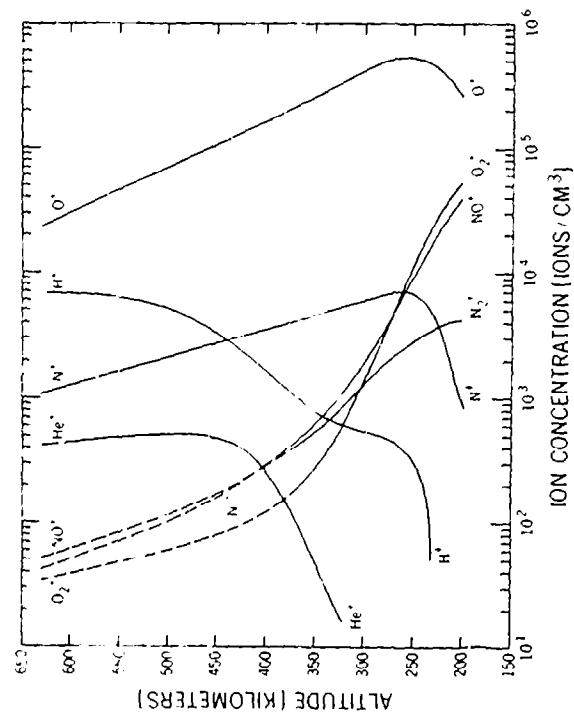


Figure 4. Altitude profiles of individual ion concentrations. The molecular ion distributions are dashed above 375 km to indicate the uncertain origin of these constituents in this altitude range.

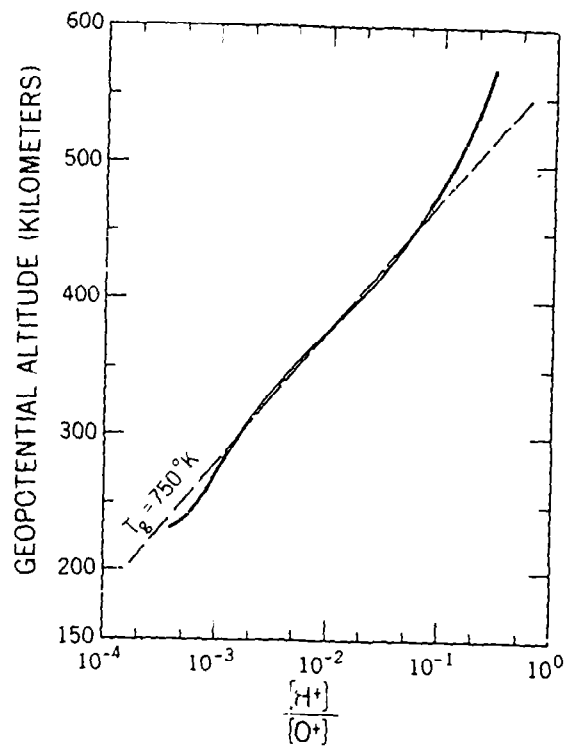


Figure 5-Variation of $\frac{[H^+]}{[O^+]}$ with geopotential altitude showing deviation from chemical equilibrium at 450 km. Slope of dashed line indicates atmospheric temperature of 750 K.

26

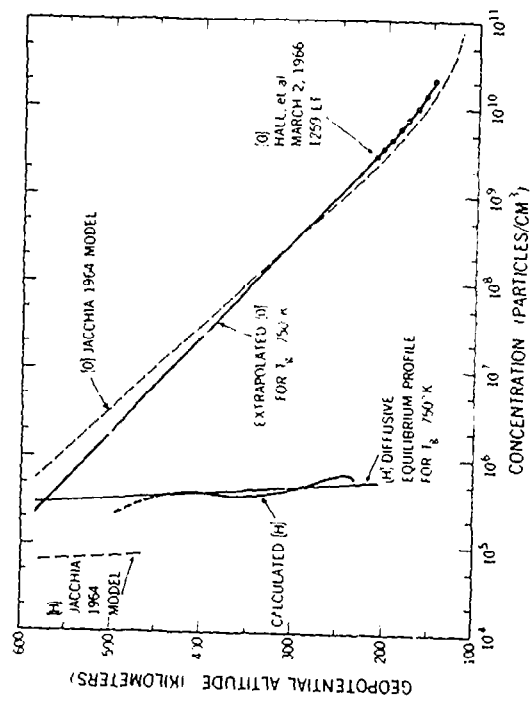


Figure 6-Calculated H^+ distribution, based on O^+ profile extrapolated from measurement of Hall et al and $\frac{[H^+]}{[O^+]}$ ratio from Figure 5. Distributions of H^+ and O^+ from Jacchia 1964 Model are shown for comparison.

27

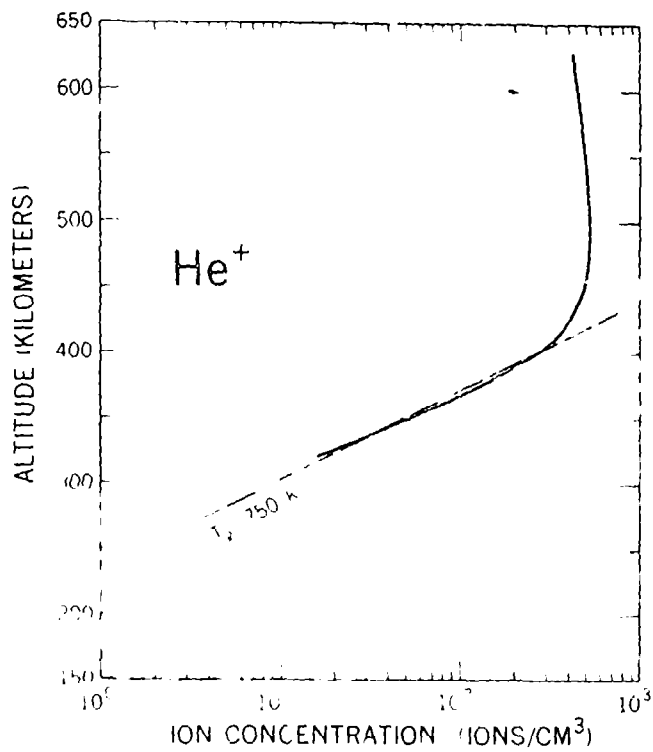


Figure 7. Altitude profile of He^+ . Slope of dashed line in chemical equilibrium region (at an isobaric temperature of 10^4 K) in agreement with estimate derived from He^+ ion data.

28

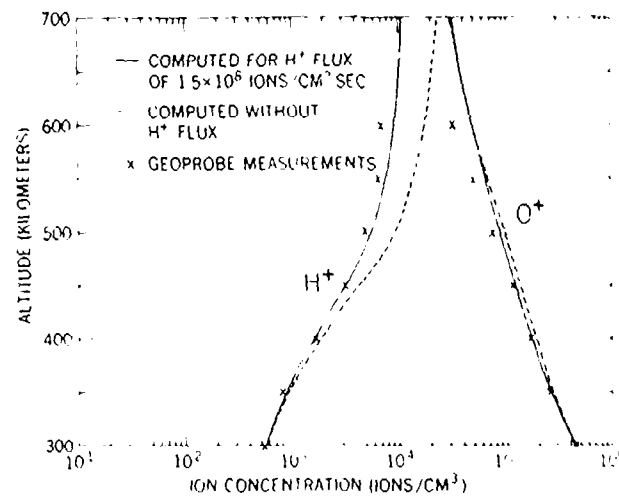


Figure 8. Distributions of H^+ and O^+ calculated by solution of continuity equations above 300 km reference level. Particle temperatures were derived from Geoprobe data of Brace et al. and a downward neutral wind $V_0 = 25 \text{ m/sec}$ was assumed (see text). An assumed, an upward flux of protons is required to fit the calculated H^+ profile to the measured points.

29